Available online at www.sciencedirect.com

ScienceDirect

IFAC PapersOnline CONFERENCE PAPER ARCHIVE

IFAC PapersOnLine 51-3 (2018) 131–136

Structure-Preserving Finite Volume Method for 2D Linear and Non-Linear Port-Hamiltonian Systems ⋆

Anass Serhani * **Denis Matignon** * **Ghislain Haine** *

* *Institut Supérieur de l'Aéronautique et de l'Espace (ISAE-Supaero), Université de Toulouse, 10 Avenue Edouard Belin, 31055 Toulouse Cedex 4, France*

anass.serhani@isae.fr denis.matignon@isae.fr ghislain.haine@isae.fr

Abstract In this work we extend the results of a high order finite volume semi-discretization for port-Hamiltonian system 1D linear case (Kotyczka (2016)) to the 2D linear case, worked on the wave equation. The existing pHs discretization methods deal only with the geometric part, in this paper we perform an adapted symplectic time stepping to get the fully discrete scheme in order to preserve both the geometrical properties and the energy aspects. We also show that staggered finite volume method carry over to a non-linear problem, the 2D irrotational shallow water equations. However, due to the non linearity and the non separability of the Hamiltonian, some difficulties arise both for the high order accuracy in the spatial discretization, and also for the symplecticity of the time integration.

Keywords: Port-Hamiltonian systems (pHs), distributed-parameter system (DPS), systems of conservation laws, structure-preserving discretization, finite volume method (FVM), symplectic integration.

1. INTRODUCTION

The analysis of physical systems is usually performed within the Lagrangian and/or Hamiltonian formalism, the modeling of physical systems based on the representation of intrinsic energy exchanges between different energetic domains allows a modular description of their (even complex) dynamic behaviour. In this context, the port-Hamiltonian framework represents a powerful modeling and control tool, see e.g. Duindam et al. (2009), Jacob and Zwart (2012), van der Schaft and Maschke (2002), van der Schaft and Jeltsema (2014). It is an ideal framework for the compositional modeling of finite- and infinite-dimensional physical systems. The port-Hamiltonian representation of open systems of conservation laws (see e.g. Le Gorrec et al. (2005), van der Schaft and Maschke (2002)) captures their physical (interconnection) structure and in particular includes the expression of boundary port variables to describe the energy exchange with the environment.

For systems of conservation laws, there exists many finite volume methods (FVM) in space (semi-discretization) or in time and space (full-discretization) with different characteristic properties to simulate various systems and application cases. An overview can be found for example in LeVeque (2002), Eymard et al. (1997), Godlewski and Raviart (1996).

⋆ This work is supported by the project ANR-16-CE92-0028, entitled *Interconnected Infinite-Dimensional systems for Heterogeneous Media*, INFIDHEM, financed by the French National Research Agency (ANR). Further information is available at https://websites.isae-supaero.fr/infidhem/the-project/

The basic idea of a fully discrete method for Hamiltonian PDEs consists of two steps. The first step consists of a spatial discretisation that reduces the PDE to a system of Hamiltonian ODEs: different structure preserving reduction methods have been suggested for linear port-Hamiltonian systems (pHs), for example, a mixed finite element scheme using simple approximation forms on every segment in Golo et al. (2004), higher order polynomials to approximate the distributed power variables at collocation points in Moulla et al. (2012), a staggered finite difference scheme in Trenchant et al. (2017), a finite volume semi-discretization based on a general leapfrog scheme in Kotyczka (2016) and more recently some methods relying on the bond forms of the pHs in Kotyczka and Maschke (2017). The second step is a time-stepping of the finite-dimensional Hamiltonian ODE using an appropriate symplectic method, which is a well-known and powerful tool that preserves the energy at the discrete time level, see e.g. Hairer et al. (2002), Leimkuhler and Reich (2004).

2. LINEAR MODEL: 2D WAVE EQUATION

2.1 Port-Hamiltonian formulation

System Consider the linear wave equation defined on the two-dimensional spatial domain $\Omega := \Omega_x \times \Omega_y$, where $\Omega_x = (0, \ell_x) \subset \mathbb{R}$ and $\Omega_y = (0, \ell_y) \subset \mathbb{R}$, and subject to boundary conditions and initial data that will be set later in the simulation section,

$$\frac{\partial^2}{\partial t^2} u(x, y, t) = \Delta u(x, y, t) \qquad \text{in } \Omega_T = \Omega \times [0, T]. \quad (1)$$

2405-8963 © 2018, IFAC (International Federation of Automatic Control) Hosting by Elsevier Ltd. All rights reserved.
Peer review under responsibility of International Federation of Automatic Control.
10.1016/j.ifacol.2018.06.037

For sake of simplicity, the values of physical coefficients are taken to 1.
Denote by

$$\mathbf{q} := \mathbf{grad}\ u = \begin{pmatrix}\partial_x u\\ \partial_y u\end{pmatrix}, \qquad p := \partial_t u. \tag{2}$$

The Hamiltonian is given by

$$\mathcal{H}(\mathbf{q},p) := \frac{1}{2}\int_0^{\ell_y}\int_0^{\ell_x} \|\mathbf{q}(x,y,t)\|^2 + p(x,y,t)^2\ dx\,dy \tag{3}$$

where $\|\cdot\|$ is the usual euclidean norm in $\mathbb{R}^2$.
We define the infinite-dimensional pHs as

$$\underbrace{\frac{\partial}{\partial t}\begin{pmatrix}\mathbf{q}\\ p\end{pmatrix}}_{f} = \underbrace{\begin{pmatrix}0 & \mathbf{grad}\\ \mathrm{div} & 0\end{pmatrix}}_{\mathcal{J}}\underbrace{\begin{pmatrix}\delta_{\mathbf{q}}\mathcal{H}\\ \delta_p\mathcal{H}\end{pmatrix}}_{e}, \tag{4}$$

where $\mathcal{J}$ is a formally skew-adjoint operator (see e.g. Kurula and Zwart (2014)) with respect to L^2 scalar product and 0 are null operator of appropriate size.
Explicitly the *flow-effort* notation is given by

$$\begin{pmatrix}f^1 & f^2 & f^3\end{pmatrix} := \begin{pmatrix}\dot{q^1} & \dot{q^2} & \dot{p}\end{pmatrix},\ \begin{pmatrix}e^1 & e^2 & e^3\end{pmatrix} := \begin{pmatrix}q^1 & q^2 & p\end{pmatrix}. \tag{5}$$

Hence

$$\begin{pmatrix}f^1\\ f^2\\ f^3\end{pmatrix} = \begin{pmatrix}0 & 0 & \partial_x\\ 0 & 0 & \partial_y\\ \partial_x & \partial_y & 0\end{pmatrix}\begin{pmatrix}e^1\\ e^2\\ e^3\end{pmatrix}. \tag{6}$$

Power balance
The derivative of the Hamiltonian along time

$$\begin{aligned}\frac{d}{dt}\mathcal{H}(\mathbf{q}(t),p(t)) &= \int_\Omega \dot{q}_1 q_1 + \dot{q}_2 q_2 + \dot{p}p\ dx\,dy\\ &= \int_{\partial\Omega}(\mathbf{q}\cdot\boldsymbol{\eta})\ p\ d\sigma, \quad (\boldsymbol{\eta}:\ \text{outward normal})\\ &= \int_0^{\ell_y} e^1(\ell_x,y)e^3(\ell_x,y) - e^1(0,y)e^3(0,y)\ dy\\ &+ \int_0^{\ell_x} e^2(x,\ell_y)e^3(x,\ell_y) - e^2(x,0)e^3(x,0)\ dx.\end{aligned}$$

This means that the energy flows through the boundary $\partial\Omega$ only. The definition of the boundary port variables f_∂ and e_∂ is chosen such that

$$\frac{d}{dt}\mathcal{H} = \langle e, f\rangle_\partial, \tag{7}$$

where $\langle .,.\rangle_\partial$ is the port-scalar product defined as

$$\langle e,f\rangle_\partial := \int_0^{\ell_y} e^T_{\partial_x} f_{\partial_x}\ dy + \int_0^{\ell_x} e^T_{\partial_y} f_{\partial_y}\ dx, \tag{8}$$

where $e_{\partial_x} := e\big|_{\partial\Omega_x\times\Omega_y}$ and $e_{\partial_y} := e\big|_{\Omega_x\times\partial\Omega_y}$ and similarly for f_{∂_x} and f_{∂_y}.

Port-boundary variables To give a general set of port-boundary variable that prove compatible with the Dirac structure and satisfy the power balance (7), we follow the proof of *Proposition 2.* in Trenchant et al. (2015) with some corrections and take into consideration the general results of Le Gorrec et al. (2005).
We split the port boundary variables into

$$f_\partial := \begin{pmatrix}f_{\partial_x}\\ f_{\partial_y}\end{pmatrix} \quad \text{and} \quad e_\partial := \begin{pmatrix}e_{\partial_x}\\ e_{\partial_y}\end{pmatrix}. \tag{9}$$

Therefore a general set of port-boundary variable is

$$\begin{pmatrix}f_{\partial_x}\\ e_{\partial_x}\end{pmatrix} = \frac{1}{\sqrt{2}}W_1\begin{pmatrix}-e^3(0,y)+e^3(\ell_x,y)\\ -e^1(0,y)+e^1(\ell_x,y)\\ e^1(0,y)+e^1(\ell_x,y)\\ e^3(0,y)+e^3(\ell_x,y)\end{pmatrix}, \tag{10}$$

$$\begin{pmatrix}f_{\partial_y}\\ e_{\partial_y}\end{pmatrix} = \frac{1}{\sqrt{2}}W_2\begin{pmatrix}-e^3(x,0)+e^3(x,\ell_y)\\ -e^2(x,0)+e^2(x,\ell_y)\\ e^2(x,0)+e^2(x,\ell_y)\\ e^3(x,0)+e^3(x,\ell_y)\end{pmatrix}, \tag{11}$$

where $W_i \in \mathbb{R}^{4\times4}$, $i\in\{1,2\}$ are matrices satisfying $W_i^T\Sigma W_i = \Sigma$, $i\in\{1,2\}$, where $\Sigma = \begin{pmatrix}0 & I\\ I & 0\end{pmatrix}$.

The Dirac structure A geometrical interpretation of (4), (10) and (11) is that the vector of flow variables f and the vector of effort variables e defined in (4) and their extension to the boundary (10)-(11) lie in a Dirac structure $\mathcal{D}$, *i.e.*$(f, f_\partial, e, e_\partial) \in \mathcal{D}$. Such $\mathcal{D}$ is a subspace of $\mathcal{F}\times\mathcal{E}$, where $\mathcal{F} = L^2(\Omega,\mathbb{R}^3)\times L^2(\partial\Omega,\mathbb{R}^4)$ is the *flow* space and $\mathcal{E} = H^1(\Omega,\mathbb{R}^3)\times L^2(\partial\Omega,\mathbb{R}^4)$ is the *effort* space.

Next we set $W_1 = W_2 = \frac{1}{\sqrt{2}}\begin{pmatrix}1 & 0 & 0 & -1\\ 1 & 0 & 0 & 1\\ 0 & -1 & 1 & 0\\ 0 & 1 & 1 & 0\end{pmatrix}$ satisfying (10) and (11), leading to

$$\begin{aligned}e_\partial &= \begin{pmatrix}e^1(0,y) & e^1(\ell_x,y) & e^2(x,0) & e^2(x,\ell_y)\end{pmatrix}^T,\\ f_\partial &= \begin{pmatrix}-e^3(0,y) & e^3(\ell_x,y) & -e^3(x,0) & e^3(x,\ell_y)\end{pmatrix}^T.\end{aligned} \tag{12}$$

These (input) port-boundary e_∂ correspond to Neumann boundary conditions for (1); indeed, with the notations (2) and (5), we get:

$$e_\partial = 0 \iff \partial_x u\big|_{\partial\Omega_x\times\Omega_y} = 0 \text{ and } \partial_y u\big|_{\Omega_x\times\partial\Omega_y} = 0. \tag{13}$$

2.2 Geometric discretization

We consider Δx (respectively Δy) the spatial step along x (respectively y), such that $x_j = j\Delta x$ and $y_l = l\Delta y$, $j\in\{0,...,N_x\}$, $l\in\{0,...,N_y\}$. We may add the assumption that we don't exceed the boundary, $x_{-\frac{1}{2}} = x_0$, $x_{N_x+\frac{1}{2}} = x_{N_x}$, $y_{-\frac{1}{2}} = y_0$ and $y_{N_y+\frac{1}{2}} = y_{N_y}$.
Let the sets of indexes $\mathcal{I}_j = \{1,...,N_x\}$, $\mathcal{I}_j^\partial = 0\cup\mathcal{I}_j$, $\mathcal{I}_l = \{1,...,N_y\}$ and $\mathcal{I}_l^\partial = 0\cup\mathcal{I}_l$. We discretize the space domain Ω into finite numbers of cells (control volume) such that,

$$\begin{aligned}\mathcal{C}^1_{jl} &:= \big(x_{j-\frac{1}{2}}, x_{j+\frac{1}{2}}\big)\times\big(y_{l-1}, y_l\big), \qquad j\in\mathcal{I}_j^\partial \quad l\in\mathcal{I}_l,\\ \mathcal{C}^2_{jl} &:= \big(x_{j-1}, x_j\big)\times\big(y_{l-\frac{1}{2}}, y_{l+\frac{1}{2}}\big), \qquad j\in\mathcal{I}_j \quad l\in\mathcal{I}_l^\partial,\\ \mathcal{C}^3_{jl} &:= \big(x_{j-1}, x_j\big)\times\big(y_{l-1}, y_l\big), \qquad j\in\mathcal{I}_j \quad l\in\mathcal{I}_l.\end{aligned}$$

We see in Figure 1 an example of three cells $\mathcal{C}^1$, $\mathcal{C}^2$, $\mathcal{C}^3$.
Denote the averaged quantities by

$$\begin{aligned}\mathcal{Q}^1_{jl} &:= \frac{1}{\Delta x\Delta y}\iint_{\mathcal{C}^1_{jl}} q^1\ dx\,dy, \qquad j\in\mathcal{I}_j^\partial \quad l\in\mathcal{I}_l,\\ \mathcal{Q}^2_{jl} &:= \frac{1}{\Delta x\Delta y}\iint_{\mathcal{C}^2_{jl}} q^2\ dx\,dy, \qquad j\in\mathcal{I}_j \quad l\in\mathcal{I}_l^\partial,\\ \mathcal{P}_{jl} &:= \frac{1}{\Delta x\Delta y}\iint_{\mathcal{C}^3_{jl}} p\ dx\,dy, \qquad j\in\mathcal{I}_j \quad l\in\mathcal{I}_l.\end{aligned} \tag{14}$$

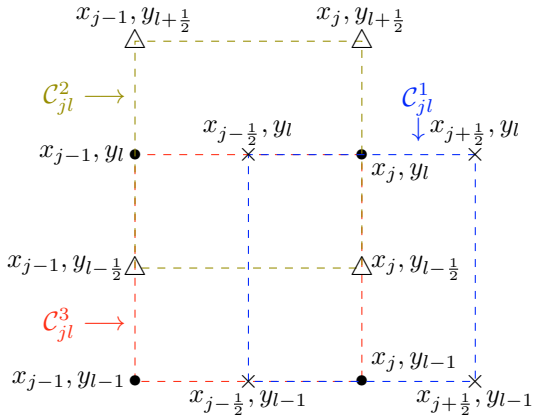

Figure 1. Example of 2D staggered cells

Therefore, we write the port-Hamiltonian system (6) in the integral form on each cell $\mathcal{C}^1_{jl}$, $\mathcal{C}^2_{jl}$ and $\mathcal{C}^3_{jl}$,

$$\frac{\partial}{\partial t}\iint_{\mathcal{C}^1_{jl}} q^1\ dx\,dy = \iint_{\mathcal{C}^1_{jl}} \frac{\partial}{\partial x}p\ dx\,dy, \tag{15}$$

$$\frac{\partial}{\partial t}\iint_{\mathcal{C}^2_{jl}} q^2\ dx\,dy = \iint_{\mathcal{C}^2_{jl}} \frac{\partial}{\partial y}p\ dx\,dy, \tag{16}$$

$$\frac{\partial}{\partial t}\iint_{\mathcal{C}^3_{jl}} p\ dx\,dy = \iint_{\mathcal{C}^3_{jl}} \frac{\partial}{\partial x}q^1\ dx\,dy + \iint_{\mathcal{C}^3_{jl}} \frac{\partial}{\partial y}q^2\ dx\,dy. \tag{17}$$

Dividing the equation (15) by $\Delta x\Delta y$ and computing explicitly the right handside first integral, $\big(j \in \mathcal{I}^{\partial}_j \quad l \in \mathcal{I}_l\big)$

$$\frac{\partial}{\partial t}\Big(\frac{1}{\Delta x\Delta y}\iint_{\mathcal{C}^1_{jl}} q^1 dx\,dy\Big) = \frac{1}{\Delta x}\Big(\underbrace{\frac{1}{\Delta y}\int_{y_{l-1}}^{y_l} p(x_{j+1/2},y)dy}_{\Phi(\mathcal{P}_{j+1,l})} - \underbrace{\frac{1}{\Delta y}\int_{y_{l-1}}^{y_l} p(x_{j-1/2},y)dy}_{\Phi(\mathcal{P}_{j,l})}\Big).$$

And similarly for the equations (16) and (17).

Natural scheme The flux on the edges of each cells can be presented as the average flux of the neighbor cell (LeVeque (2002), Godlewski and Raviart (1996)). Then the approximated flux is the natural one, i.e. $\Phi: u \mapsto u$. Hence, equations (15)-(17) can be written as

$$\begin{aligned}
\dot{\mathcal{Q}}^1_{jl} &= \frac{1}{\Delta x}\Big(\Phi(\mathcal{P}_{j+1,l}) - \Phi(\mathcal{P}_{j,l})\Big),\\
\dot{\mathcal{Q}}^2_{jl} &= \frac{1}{\Delta y}\Big(\Phi(\mathcal{P}_{j,l+1}) - \Phi(\mathcal{P}_{j,l})\Big),\\
\dot{\mathcal{P}}_{jl} &= \frac{\Phi(\mathcal{Q}^1_{j,l}) - \Phi(\mathcal{Q}^1_{j-1,l})}{\Delta x} + \frac{\Phi(\mathcal{Q}^2_{j,l}) - \Phi(\mathcal{Q}^2_{j,l-1})}{\Delta y}.
\end{aligned}$$

By writing the flux Φ explicitly and by adopting the notation $\mathcal{Q}^1_{\partial_x} := \big(\mathcal{Q}^1_{0,1},...,\mathcal{Q}^1_{0,N_y},\mathcal{Q}^1_{N_x,1},...,\mathcal{Q}^1_{Nx,N_y}\big)$ and similarly for $\mathcal{Q}^2_{\partial_y}$, $\mathcal{P}_{\partial_x}$ and $\mathcal{P}_{\partial_y}$, we get a semi-discrete FVM for the pHs outcome from the 2D wave equation:

$$\begin{cases}
\begin{pmatrix}\dot{\mathcal{Q}}^1\\ \dot{\mathcal{Q}}^2\\ \dot{\mathcal{P}}\end{pmatrix} = \underbrace{\begin{pmatrix}0 & 0 & D_1\\ 0 & 0 & \tilde{D}_1\\ -D_1^T & -\tilde{D}_1^T & 0\end{pmatrix}}_{J_1^d}\begin{pmatrix}\mathcal{Q}^1\\ \mathcal{Q}^2\\ \mathcal{P}\end{pmatrix} + \underbrace{\begin{pmatrix}0 & 0\\ g_1 & \tilde{g}_1\end{pmatrix}}_{g_1^d}\begin{pmatrix}Q^1_{\partial_x}\\ Q^2_{\partial_y}\end{pmatrix},\\
\begin{pmatrix}\mathcal{P}_{\partial_x}\\ \mathcal{P}_{\partial_y}\end{pmatrix} = \begin{pmatrix}0 & 0\\ g_1 & \tilde{g}_1\end{pmatrix}^T\begin{pmatrix}\mathcal{Q}^1\\ \mathcal{Q}^2\\ \mathcal{P}\end{pmatrix},
\end{cases}$$

where,

$D_1 \in \mathbb{R}^{(N_x-1)N_y\times N_xN_y}$, $\tilde{D} \in \mathbb{R}^{N_x(N_y-1)\times N_xN_y}$, $A_1 \in \mathbb{R}^{(N_y-1)N_y}$, $g_1 \in \mathbb{R}^{N_xN_y\times 2N_y}$, $\tilde{g}_1 \in \mathbb{R}^{N_xN_y\times 2N_x}$, $B \in \mathbb{R}^{N_y\times 2}$,

$$D_1 = \frac{1}{\Delta x}\begin{pmatrix}-1 & 0 & \cdots & 0 & 1 & 0 & \cdots & 0\\ 0 & \ddots & \ddots & & \ddots & \ddots & \ddots & \vdots\\ \vdots & \ddots & \ddots & \ddots & & \ddots & \ddots & 0\\ 0 & \cdots & 0 & -1 & 0 & \cdots & 0 & 1\end{pmatrix},$$

$$\tilde{D}_1 = \frac{1}{\Delta y}\begin{pmatrix}A_1 & & \\ & \ddots & \\ & & A_1\end{pmatrix},\quad \text{where } A_1 = \begin{pmatrix}-1 & 1 & \\ & \ddots & \ddots\\ & & -1\ 1\end{pmatrix},$$

$$g_1 = \frac{1}{\Delta x}\begin{pmatrix}-I_{N_y} & 0\\ 0 & \vdots\\ \vdots & 0\\ 0 & I_{N_y}\end{pmatrix},\quad \tilde{g}_1 = \frac{1}{\Delta y}\begin{pmatrix}B & & \\ & \ddots & \\ & & B\end{pmatrix},\quad B = \begin{pmatrix}-1 & 0\\ 0 & \vdots\\ \vdots & 0\\ 0 & 1\end{pmatrix}.$$

General leapfrog scheme Until now, we have worked with a natural flux, meaning that the flux takes only the average of neighbor cell. The results presented for the 1D case in Kotyczka (2016), making use of Iserles (1986) and Fornberg and Ghrist (1999), are extended to a general finite volume leapfrog scheme for the two-dimensional pHs. Then the general leapfrog flux takes r components on each side (in both direction x and y). As a consequence the equations (15), (16) and (17) can be presented as

$$\begin{aligned}
\dot{\mathcal{Q}}^1_{jl} &= \frac{1}{\Delta x}\Big(\Phi(\mathcal{P}_{j+1,l},...,\mathcal{P}_{j+r,l}) - \Phi(\mathcal{P}_{j,l},...,\mathcal{P}_{j-r+1,l})\Big),\\
\dot{\mathcal{Q}}^2_{jl} &= \frac{1}{\Delta y}\Big(\Phi(\mathcal{P}_{j,l+1},...,\mathcal{P}_{j,l+r}) - \Phi(\mathcal{P}_{j,l},...,\mathcal{P}_{j,l-r+1})\Big),\\
\dot{\mathcal{P}}_{jl} &= \frac{1}{\Delta x}\Big(\Phi(\mathcal{Q}^1_{j,l},...,\mathcal{Q}^1_{j+r-1,l}) - \Phi(\mathcal{Q}^1_{j-1,l},...,\mathcal{Q}^1_{j-r,l})\Big)\\
&\quad + \frac{1}{\Delta y}\Big(\Phi(\mathcal{Q}^2_{j,l},...,\mathcal{Q}^2_{j,l+r-1}) - \Phi(\mathcal{Q}^2_{j,l-1},...,\mathcal{Q}^2_{j,l-r})\Big).
\end{aligned}$$

The flux Φ now depends on r neighbor components,

$$\Phi: (u_1,...,u_r) \mapsto \sum_{n=1}^{r} a_{r,n}u_n. \tag{18}$$

Notice the right value of the coefficients $a_{r,n}$, compared to Kotyczka (2016):

$$a_{r,n} = (-1)^{n-1}\frac{1}{2(n-\frac{1}{2})^2}\ \frac{\big((2r-1)!!\big)^2}{\big(2r-1-2(n-\frac{1}{2})\big)!!\ \big(2r-1+2(n-\frac{1}{2})\big)!!}, \tag{19}$$

we refer to (Fornberg and Ghrist (1999)) for the proof. For higher order ($r \geq 2$), we see that the indexes exceed the boundaries of both axis along x and y, thus following LeVeque (2002) we add so-called *ghost cells*,

$$\begin{aligned}
&\mathcal{Q}^1_{j<0,l} := \mathcal{Q}^1_{0,l}, \quad \mathcal{Q}^1_{j>N_x,l} := \mathcal{Q}^1_{N_x,l}, \quad l \in \mathcal{I}_l\\
&\mathcal{Q}^2_{j,l<0} := \mathcal{Q}^2_{j,0}, \quad \mathcal{Q}^2_{j,l>N_y} := \mathcal{Q}^2_{j,N_y}, \quad j \in \mathcal{I}_j\\
&\mathcal{P}_{j>N_x,l} := 0, \quad \mathcal{P}_{j<1,l} := 0, \quad l \in \mathcal{I}_l\\
&\mathcal{P}_{j,l>N_y} := 0, \quad \mathcal{P}_{j,l<1} := 0, \quad j \in \mathcal{I}_j
\end{aligned} \tag{20}$$

Hence, a semi-discrete FVM with a general leapfrog scheme reads:

$$\begin{cases} \dot{\mathcal{Q}}^1_{jl} = \dfrac{1}{\Delta x}\displaystyle\sum_{n=1}^{r} a_{r,n}\Big(\mathcal{P}_{j+n,l} - \mathcal{P}_{j-n+1,l}\Big), \\ \dot{\mathcal{Q}}^2_{jl} = \dfrac{1}{\Delta y}\displaystyle\sum_{n=1}^{r} a_{r,n}\Big(\mathcal{P}_{j,l+n} - \mathcal{P}_{j,l-n+1}\Big), \\ \dot{\mathcal{P}}_{jl} = \dfrac{1}{\Delta x}\displaystyle\sum_{n=1}^{r} a_{r,n}\Big(\mathcal{Q}^1_{j+n-1,l} - \mathcal{Q}^1_{j-n,l}\Big) \\ \qquad\qquad + \dfrac{1}{\Delta y}\displaystyle\sum_{r=1}^{n} a_{r,n}\Big(\mathcal{Q}^2_{j,l+n-1} - \mathcal{Q}^2_{j,l-n}\Big). \end{cases} \tag{21}$$

With $\mathcal{Q}^1_{\partial_x}$, $\mathcal{Q}^2_{\partial_y}$ the boundary averaged quantities respectively on $\partial\Omega_x$ and $\partial\Omega_y$, we can write (21) in matrix form as

$$\begin{cases} \begin{pmatrix} \dot{\mathcal{Q}}^1 \\ \dot{\mathcal{Q}}^2 \\ \dot{\mathcal{P}} \end{pmatrix} = \underbrace{\begin{pmatrix} 0 & 0 & D_r \\ 0 & 0 & \tilde{D}_r \\ -D_r^T & -\tilde{D}_r^T & 0 \end{pmatrix}}_{J_r^d} \begin{pmatrix} \mathcal{Q}^1 \\ \mathcal{Q}^2 \\ \mathcal{P} \end{pmatrix} + \underbrace{\begin{pmatrix} 0 & 0 \\ g_r & \tilde{g}_r \end{pmatrix}}_{g_r^d} \begin{pmatrix} \mathcal{Q}^1_{\partial_x} \\ \mathcal{Q}^2_{\partial_y} \end{pmatrix}, \\ \begin{pmatrix} \mathcal{P}_{\partial_x} \\ \mathcal{P}_{\partial_y} \end{pmatrix} = \begin{pmatrix} 0 & 0 \\ g_r & \tilde{g}_r \end{pmatrix}^T \begin{pmatrix} \mathcal{Q}^1 \\ \mathcal{Q}^2 \\ \mathcal{P} \end{pmatrix}, \end{cases} \tag{22}$$

where

$D_r \in \mathbb{R}^{(N_x-1)N_y \times N_x N_y}$, $\tilde{D}_r \in \mathbb{R}^{N_x(N_y-1)\times N_x N_y}$, $A_r \in \mathbb{R}^{(N_y-1)N_y}$ $g_r \in \mathbb{R}^{N_x N_y \times 2N_y}$, $B_n \in \mathbb{R}^{N_y \times N_y}$, $\tilde{g}_r \in \mathbb{R}^{N_x N_y \times 2N_x}$, $C_r \in \mathbb{R}^{N_y \times 2}$, are given by

$$D_r = \frac{1}{\Delta x}\begin{pmatrix} -a_{r,1} & 0 & \cdots & 0 & a_{r,1} & \cdots & a_{r,r} & & \\ \vdots & \ddots & \ddots & & \ddots & \ddots & & \ddots & \\ -a_{r,r} & & \ddots & \ddots & & \ddots & \ddots & & a_{r,r} \\ & \ddots & & \ddots & \ddots & & \ddots & \ddots & \vdots \\ & & -a_{r,r} & \cdots & -a_{r,1} & 0 & \cdots & 0 & a_{r,1} \end{pmatrix},$$

$$\tilde{D}_r = \frac{1}{\Delta y}\begin{pmatrix} A_r & & \\ & \ddots & \\ & & A_r \end{pmatrix}, \quad A_r = \begin{pmatrix} -a_{r,1} & a_{r,1} & \cdots & a_{r,r} & & \\ \vdots & \ddots & \ddots & & \ddots & \\ -a_{r,r} & & \ddots & \ddots & & a_{r,r} \\ & \ddots & & \ddots & \ddots & \vdots \\ & & -a_{r,r} & \cdots & -a_{r,1} & a_{r,1} \end{pmatrix},$$

$$g_r = \frac{1}{\Delta x}\begin{pmatrix} -B & 0 \\ 0 & \mathrm{flip}(B) \end{pmatrix}, \quad B = \begin{pmatrix} B_1 \\ \vdots \\ B_r \end{pmatrix}, \quad B_n = b_n I_{N_y},\ b_n = \sum_{i=n}^{r} a_{r,i},$$

$$\tilde{g}_r = \frac{1}{\Delta y}\begin{pmatrix} C_r & & \\ & \ddots & \\ & & C_r \end{pmatrix}, \quad C_r = \begin{pmatrix} -b_1 & 0 \\ \vdots & \vdots \\ -b_r & 0 \\ 0 & b_r \\ \vdots & \vdots \\ 0 & b_1 \end{pmatrix}, \quad b_n = \sum_{i=n}^{r} a_{r,i}.$$

where $\mathrm{flip}(B) := \big(B_r, ..., B_1\big)^T$.

Remark The matrices D_r and $\tilde{D}_r$ are Toeplitz matrices which remain of the same size as D_1 whatever r, but the higher the order of accuracy r, the more dense (or less sparse) the matrices D_r and $\tilde{D}_r$.

Then the associated discrete Hamiltonian is given by

$$\mathcal{H}_d := \frac{1}{2}\sum_{i,j}\Big(\big(\mathcal{Q}^1_{ij}\big)^2 + \big(\mathcal{Q}^2_{ij}\big)^2 + \big(\mathcal{P}_{ij}\big)^2\Big)\Delta x \Delta y \tag{23}$$

Making use of the discrete *flow-effort* notation given by

$$F_d = \begin{pmatrix} \dot{\mathcal{Q}}^1 \\ \dot{\mathcal{Q}}^2 \\ \dot{\mathcal{P}} \end{pmatrix},\ E_d = \begin{pmatrix} \mathcal{Q}^1 \\ \mathcal{Q}^2 \\ \mathcal{P} \end{pmatrix},\ F_d^\partial = \begin{pmatrix} \mathcal{P}_{\partial_x} \\ \mathcal{P}_{\partial_y} \end{pmatrix},\ E_d^\partial = \begin{pmatrix} \mathcal{Q}^1_{\partial_x} \\ \mathcal{Q}^2_{\partial_y} \end{pmatrix},$$

a compact form of the discrete pHs (22) is obtained:

$$\begin{cases} F_d = J_r^d E_d + g_r^d E_d^\partial, \\ F_d^\partial = {g_r^d}^T E_d. \end{cases} \tag{24}$$

The power balance mimicking (7) is

$$F_d(t)^T\, E_d(t) = F_d^\partial(t)^T\, E_d^\partial(t)\,. \tag{25}$$

Numerical results Consider system (6) with boundary conditions (12), the angular frequencies of the infinite-dimensional skew-adjoint operator $(\mathcal{J}, D(\mathcal{J}))$,

$$\omega_{m,n} = \pi\sqrt{\Big(\frac{m}{\ell_x}\Big)^2 + \Big(\frac{n}{\ell_y}\Big)^2}, \qquad m, n \in \mathbb{N}.$$

Figure 2 illustrates the comparison between the angular frequencies of the operator $(\mathcal{J}, D(\mathcal{J}))$ and the eigenvalues of the matrix J_r^d with different values of r, we set $N_x = N_y = 10$ and $\ell_x = \ell_y = 1$, with $r = 1, 2, 3, 6$. We see that the higher the consistence order r, the closer the discrete angular frequencies to the exact ones.

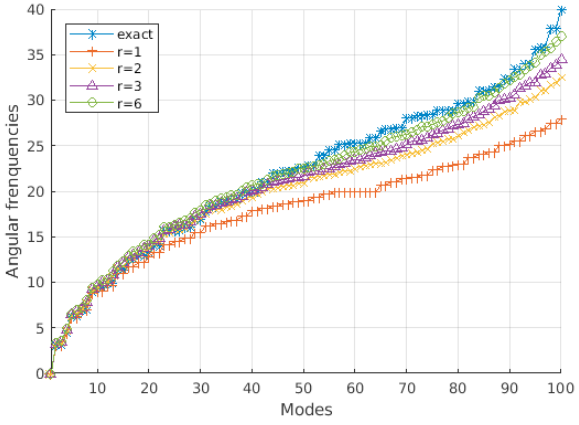

Figure 2. Exact angular frequencies of $\mathcal{J}$ compared to eigenvalues of J_r^d for different orders of accuracy r.

2.3 Time integration

We studied a finite volume semi-discretization that preserves the geometric structure. In addition, we now seek for a full discretization of the problem, so we perform a time stepping scheme. Since we are dealing with Hamiltonians, we look for schemes that preserve the Hamiltonian along time, hence, we use symplectic schemes as *symplectic Euler* (order 1), *Störmer-Verlet* (order 2) schemes or *Lobatto IIIA-IIIB Pairs* (order 4).

We discretize the time interval $[0, T]$ uniformly with the step Δt such that $N_t \Delta t = T$. Then denote by $\mathcal{Q}^{1(k)}_{jl} := \mathcal{Q}_{ij}(k\Delta t)$, and similarly for $\mathcal{Q}^{2(k)}_{jl}$, $\mathcal{P}^k_{jl}$ and $\mathcal{H}^k_d := \mathcal{H}_d(k\Delta t)$. The symplectic Euler scheme adapted to finite volume scheme is of order 1 in Δt, and reads:

$$\begin{cases} \mathcal{Q}^{1(k+1)}_{jl} = \mathcal{Q}^{1(k)}_{jl} + \dfrac{\Delta t}{\Delta x}\displaystyle\sum_{n=1}^{r} a_{n,r}\Big(\mathcal{P}^{k}_{j+n,l} - \mathcal{P}^{k}_{j-n+1,l}\Big), \\ \mathcal{Q}^{2(k+1)}_{jl} = \mathcal{Q}^{2(k)}_{jl} + \dfrac{\Delta t}{\Delta y}\displaystyle\sum_{n=1}^{r} a_{n,r}\Big(\mathcal{P}^{k}_{j,l+n} - \mathcal{P}^{k}_{j,l-n+1}\Big), \\ \mathcal{P}^{k+1}_{jl} = \mathcal{P}^{k}_{jl} + \dfrac{\Delta t}{\Delta x}\displaystyle\sum_{n=1}^{r} a_{n,r}\Big(\mathcal{Q}^{1(k+1)}_{j+n-1,l} - \mathcal{Q}^{1(k+1)}_{j-n,l}\Big) \\ \qquad\qquad + \dfrac{\Delta t}{\Delta y}\displaystyle\sum_{n=1}^{r} a_{n,r}\Big(\mathcal{Q}^{2(k+1)}_{j,l+n-1} - \mathcal{Q}^{2(k+1)}_{j,l-n}\Big). \end{cases}$$

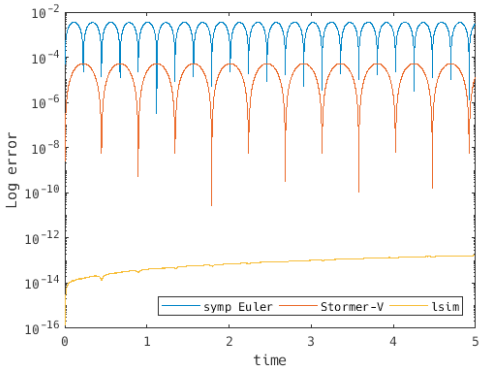

Figure 3. The Hamiltonian relative error $\mathcal{H}^k_d$

Figure 3 shows the relative error, on the initial discrete Hamiltonian value ($|\frac{\mathcal{H}^0_d - \mathcal{H}^k_d}{\mathcal{H}^0_d}|$), of the three different time integration schemes; symplectic Euler (order 1), Störmer-Verlet (order 2) and *lsim* (not symplectic), on a logarithmic scale. The two symplectic schemes keep a bounded oscillatory behaviour along time, however the *lsim*'s relative error, even if it is very small, is increasing over time due to the non-symplecticity. Note that instability can occur if a CFL condition is not fulfilled.

More details on the computations and further simulation results are sketched in Serhani (2017).

3. NON-LINEAR MODEL: IRROTATIONAL 2D SHALLOW WATER EQUATIONS

3.1 Port-Hamiltonian formulation

We now consider the irrotational shallow water equations (SWE) on the two-dimensional space $\Omega := \Omega_x \times \Omega_y = (-a, a) \times (-b, b)$, and with $\mathbf{u}$ is the velocity vector and h is the height profile ($h > 0$),

$$\begin{cases} \dfrac{\partial h}{\partial t} + \operatorname{div}(h\mathbf{u}) = 0, \\ \dfrac{\partial \mathbf{u}}{\partial t} + \mathbf{grad}\big(\dfrac{1}{2}\|\mathbf{u}\|^2 + gh\big) = 0, \end{cases} \tag{26}$$

where g is the gravity constant. Note that another discretization method of this PDE system has recently been considered in Kotyczka and Maschke (2017) by making use of primal and dual grids.
Denote by

$$q := h \quad \text{and} \quad \mathbf{p} := \rho\mathbf{u} = \rho\begin{pmatrix} u_x \\ u_y \end{pmatrix}, \tag{27}$$

where ρ is the mass density.
Hence we can write the Hamiltonian as

$$\mathcal{H}(q, \mathbf{p}) = \frac{1}{2}\int_\Omega \Big(\frac{1}{\rho}\ q\ \|\mathbf{p}\|^2\ +\ \rho\ g\ q^2\Big)\ dx\, dy \tag{28}$$

Then the variational derivatives are

$$\frac{\delta \mathcal{H}}{\delta q} = \frac{1}{2\rho}\|\mathbf{p}\|^2 + \rho g q \quad \text{and} \quad \frac{\delta \mathcal{H}}{\delta \mathbf{p}} = \frac{1}{\rho}q\mathbf{p}. \tag{29}$$

The quantities $\delta_q\mathcal{H}$ and $\delta_{\mathbf{p}}\mathcal{H}$ are respectively the hydrodynamic pressure and the water flow.
Then (26) can be written as

$$\frac{\partial}{\partial t}\begin{pmatrix} q \\ \mathbf{p} \end{pmatrix} = \underbrace{\begin{pmatrix} 0 & -\operatorname{div} \\ -\mathbf{grad} & 0 \end{pmatrix}}_{\mathcal{J}}\begin{pmatrix} \delta_q\mathcal{H} \\ \delta_{\mathbf{p}}\mathcal{H} \end{pmatrix}, \tag{30}$$

where $\mathcal{J}$ is a formally skew-adjoint operator, then

$$\begin{pmatrix} f^1 \\ f^2 \\ f^3 \end{pmatrix} = \begin{pmatrix} 0 & -\partial_x & -\partial_y \\ -\partial_x & 0 & 0 \\ -\partial_y & 0 & 0 \end{pmatrix}\begin{pmatrix} e^1 \\ e^2 \\ e^3 \end{pmatrix}. \tag{31}$$

And by making use of ***flow-effort*** notations we get

$$f := \begin{pmatrix} f^1 \\ f^{\{2,3\}} \end{pmatrix} := \frac{\partial}{\partial t}\begin{pmatrix} q \\ \mathbf{p} \end{pmatrix} \text{ and } e := \begin{pmatrix} e^1 \\ e^{\{2,3\}} \end{pmatrix} := \begin{pmatrix} \delta_q\mathcal{H} \\ \delta_{\mathbf{p}}\mathcal{H} \end{pmatrix}.$$

The power balance Taking the time-derivative of the Hamiltonian, we get

$$\frac{d}{dt}\mathcal{H}(q(t), \mathbf{p}(t)) = \int_{\partial\Omega} -e^1\ \big(e^{\{2,3\}} \cdot \boldsymbol{\eta}\big)\ d\sigma. \tag{32}$$

Since Ω is a Cartesian domain, we have

$$\begin{aligned} \frac{d}{dt}\mathcal{H} = &\int_{-b}^{b} -e^1(a,y)e^2(a,y) + e^1(-a,y)e^2(-a,y)\ dy \\ &+ \int_{-a}^{a} -e^1(x,b)e^3(x,b) + e^1(x,-b)e^3(x,-b)\ dx \end{aligned}$$

Then the input-output variables can be chosen such that (7) holds, with definitions (10) and (11). And for the next semi-discretization we set,

$$\begin{aligned} e_\partial &= \big(e^2(-a,y)\ e^2(a,y)\ e^3(x,-b)\ e^3(x,b)\big)^T, \\ f_\partial &= \big(-e^1(-a,y)\ e^1(a,y)\ -e^1(x,-b)\ e^1(x,b)\big)^T. \end{aligned} \tag{33}$$

Note that the port-variables (33) are such a non-linear combination of Dirichlet boundary conditions of (26), for example

$$e_\partial = 0 \iff hu_x\big|_{\partial\Omega_x\times\Omega_y} = 0 \text{ and } hu_y\big|_{\Omega_x\times\partial\Omega_y} = 0,$$

meaning that the water flow is equal to zero on each corresponding boundary.

The Dirac structure A geometrical interpretation of (31) and (33) is that the vector of flow variables f and the vector of effort variables e defined in (31) and their extension to the boundary (33) lie in a Dirac structure $\mathcal{D}$, *i.e.* $(f, f_\partial, e, e_\partial) \in \mathcal{D}$.

3.2 Geometric discretization

Taking in consideration the same domain discretization principle as in *Section 2.2* for Ω, we consider the cells,

$$\begin{aligned} \mathcal{C}^1_{jl} &= \big(x_{j-1}, x_j\big) \times \big(y_{l-1}, y_l\big), && j \in \mathcal{I}_j, \quad l \in \mathcal{I}_l \\ \mathcal{C}^2_{jl} &= \big(x_{j-\frac{1}{2}}, x_{j+\frac{1}{2}}\big) \times \big(y_{l-1}, y_l\big), && j \in \mathcal{I}^\partial_j, \quad l \in \mathcal{I}_l \\ \mathcal{C}^3_{jl} &= \big(x_{j-1}, x_j\big) \times \big(y_{l-\frac{1}{2}}, y_{l+\frac{1}{2}}\big), && j \in \mathcal{I}_j, \quad l \in \mathcal{I}^\partial_l \end{aligned}$$

We project the integral form of pHs (31) over the discretized cells, and following the steps of *Section 2.2* and adopting the notations of the discrete flow end effort averaged quantities, with $\alpha, \beta = 1, 2, 3$:

$$F^{\alpha}_{j,l} := \frac{1}{\Delta x \Delta y} \iint_{\mathcal{C}^{\alpha}_{jl}} f^{\alpha}\, dx\, dy,\ E^{\beta}_{j,l} := \frac{1}{\Delta x \Delta y} \iint_{\mathcal{C}^{\beta}_{jl}} e^{\beta}\, dx\, dy,$$

we get a structure-preserving FVM for the 2D SWE,

$$\begin{aligned} F^1_{j,l} &= -\frac{1}{\Delta x}\big(E^2_{j,l} - E^2_{j-1,l}\big) - \frac{1}{\Delta y}\big(E^3_{j,l} - E^3_{j,l-1}\big), \\ F^2_{j,l} &= -\frac{1}{\Delta x}\big(E^1_{j+1,l} - E^1_{j,l}\big), \\ F^3_{j,l} &= -\frac{1}{\Delta y}\big(E^1_{j,l+1} - E^1_{j,l}\big). \end{aligned} \tag{34}$$

Then a discrete form of the pHs (31) is:

$$\begin{cases} \begin{pmatrix} F^1_d \\ F^2_d \\ F^3_d \end{pmatrix} = \underbrace{\begin{pmatrix} 0 & -D_1^T & -\tilde{D}_1^T \\ D_1 & 0 & 0 \\ \tilde{D}_1 & 0 & 0 \end{pmatrix}}_{J^d_1} \begin{pmatrix} E^1_d \\ E^2_d \\ E^3_d \end{pmatrix} + \underbrace{\begin{pmatrix} 0 & 0 \\ g_1 & \tilde{g}_1 \end{pmatrix}}_{g^d_1} E^{\partial}_d, \\ F^{\partial}_d = \begin{pmatrix} 0 & 0 \\ g_1 & \tilde{g}_1 \end{pmatrix}^T \begin{pmatrix} E^1_d \\ E^2_d \\ E^3_d \end{pmatrix}, \end{cases} \tag{35}$$

which can be written in compact form as in (24), with the discrete power balance given in (25).

Remark We see that (24) (with $r = 1$) and (35) share a similar discrete *flow-effort* structure. Indeed, they have exactly the same discrete *flows*, which is the time derivative of the state variables. However, the discrete *efforts* have different definitions depending on the PDE under consideration: for the wave equation, since the Hamiltonian is quadratic (separable) the *effort* variables are exactly the state variables or a linear combination of them (in the case of physical coefficients being different from 1 in the Hamiltonian (3)). However for SWE, the Hamiltonian is non-linear and not separable, then the *effort* variables are a non-linear combination of the state variables.

3.3 Discussion

Several open questions can be raised:

(1) The extension of the method to higher spatial accuracy doesn't easily carry over due to the non-linearity, at each space step a Riemann problem should be solved to achieve stability and consistency.
(2) The computation of the discrete Hamiltonian $\mathcal{H}_d(t)$ associated to (35) is not straightforward contrarily to (23). The definition proposed in Kotyczka and Maschke (2017) could be further investigated for our framework.
(3) After a structure-preserving semi-discretization that fits the geometric properties of the Hamiltonian, we look for an adapted symplectic time integration, that shares the energy conservation characteristic along time. However, since the Hamiltonian is non-separable and non-linear, two issues arise: first, *any symplectic scheme will be necessarily implicit*, this is due to the non-separablity (see e.g. Hairer et al. (2002)). Second, the non-linearity leads to *the resolution of a non-linear system at each time step*. In order to overcome this problem, following e.g. (Leimkuhler and Reich, 2004, chap. 6), we could use *Partitioned Runge-Kutta* methods with multiple stages and orders for the nonlinear Hamiltonian ODE associated to (35).

REFERENCES

Duindam, V., Macchelli, A., Stramigioli, S., and Bruyninckx, H. (2009). *Modeling and Control of Complex Physical Systems*. Springer.

Eymard, R., Galloüet, T., and Herbin, R. (1997). *Finite Volume Methods*. Handbook of Numerical Analysis.

Fornberg, B. and Ghrist, M. (1999). Spatial finite difference approximations for wave-type equations. *SIAM Journal on Numerical Analysis*, 37, 105–130.

Godlewski, E. and Raviart, P.A. (1996). *Numerical Approximation of Hyperbolic Systems of Conservation Laws*. Springer.

Golo, G., Talasila, V., Van der Schaft, A., and Maschke, B. (2004). Hamiltonian discretization of boundary control systems. *Automatica*, 40, 757–771.

Hairer, E., Lubich, C., and Wanner, G. (2002). *Geometric Numerical Integration: Structure-Preserving Algorithms for Ordinary Differential Equations*. Spinger.

Iserles, A. (1986). Generalized leapfrog methods. *IMA Journal of Numerical Analysis*, 6, 381–392.

Jacob, B. and Zwart, H. (2012). *Linear Port-Hamiltonian Systems on Infinite-dimensional Spaces*. Birkhauser.

Kotyczka, P. and Maschke, B. (2017). Discrete port-Hamiltonian formulation and numerical approximation for systems of two conservation laws. *at - Automatisierungstechnik*, 65(5).

Kotyczka, P. (2016). Finite volume structure-preserving discretization of 1d distributed-parameter port-Hamiltonian systems. *IFAC-PapersOnLine*, 49, 298–303.

Kurula, M. and Zwart, H. (2014). Linear wave systems on n-D spatial domains. *International Journal of Control*, 88, 1063–1077.

Le Gorrec, Y., Zwart, H., and Maschke, B. (2005). Dirac structures and boundary control systems associated with skew-symmetric differential operators. *SIAM Journal on Control and Optimization*, 1864–1892.

Leimkuhler, B. and Reich, S. (2004). *Simulating Hamiltonian Dynamics*. Cambridge University Press.

LeVeque, R.J. (2002). *Finite Volume Methods for Hyperbolic Problems*. Cambridge University Press.

Moulla, R., Lefèvre, L., and Maschke, B. (2012). Pseudo-spectral methods for the spatial symplectic reduction of open systems of conservation laws. *Journal of Computational Physics*, 1272–1292.

Serhani, A. (2017). *Geometric discretization methods for hyperbolic systems, and link with finite volume methods for conservation laws*. Master 2 Thesis, University of Limoges. URL `https://www.researchgate.net/publication/323245189_Geometric_discretization_methods_for_hyperbolic_systems_and_link_with_finite_volume_methods_for_conservation_laws`.

Trenchant, V., Fares, Y., Ramirez, H., Le Gorrec, Y., and Ouisse, M. (2015). A port-Hamiltonian formulation of a 2D boundary controlled acoustic system. *IFAC-PapersOnLine*, 48, 235–240.

Trenchant, V., Ramirez Estay, H., Le Gorrec, Y., and Paul, K. (2017). Structure preserving spatial discretization of 2d hyperbolic systems using staggered grids finite difference. The 2017 American Control conference, Seattle, USA.

van der Schaft, A. and Jeltsema, D. (2014). *Port-Hamiltonian Systems Theory: An Introductory Overview*. Foundation and Trends in Systems and Control.

van der Schaft, A. and Maschke, B. (2002). Hamiltonian formulation of distributed-parameter systems with boundary energy flow. *Journal of Geometry and Physics*, 42, 166–196.